Protein Science (2000), *9*:2528–2534. Cambridge University Press. Printed in the USA.

Rationale for Bcl-x_L/Bad peptide complex formation from structure, mutagenesis, and biophysical studies

ANDREW M. PETROS,[1] DAVID G. NETTESHEIM,[1] YI WANG,[1] EDWARD T. OLEJNICZAK,[1] ROBERT P. MEADOWS,[1] JAMEY MACK,[1] KERRY SWIFT,[1] EDMUND D. MATAYOSHI,[1] HAICHAO ZHANG,[1] CRAIG B. THOMPSON,[2] AND STEPHEN W. FESIK[1]

[1]Pharmaceutical Discovery Division, Abbott Laboratories, Abbott Park, Illinois 60064
[2]Abramson Family Cancer Research Institute, University of Pennsylvania, Philadelphia, Pennsylvania 19104

(RECEIVED August 1, 2000; FINAL REVISION October 2, 2000; ACCEPTED October 3, 2000)

Abstract

The three-dimensional structure of the anti-apoptotic protein Bcl-x_L complexed to a 25-residue peptide from the death promoting region of Bad was determined using NMR spectroscopy. Although the overall structure is similar to Bcl-x_L bound to a 16-residue peptide from the Bak protein (Sattler et al., 1997), the Bad peptide forms additional interactions with Bcl-x_L. However, based upon site-directed mutagenesis experiments, these additional contacts do not account for the increased affinity of the Bad 25-mer for Bcl-x_L compared to the Bad 16-mer. Rather, the increased helix propensity of the Bad 25-mer is primarily responsible for its greater affinity for Bcl-x_L. Based on this observation, a pair of 16-residue peptides were designed and synthesized that were predicted to have a high helix propensity while maintaining the interactions important for complexation with Bcl-x_L. Both peptides showed an increase in helix propensity compared to the wild-type and exhibited an enhanced affinity for Bcl-x_L.

Keywords: Bad protein; Bcl-x_L; helix propensity; NMR spectroscopy

The Bcl-2 family of proteins are important regulators of programmed cell death. Some members of this family (e.g., Bax, Bak, and Bid) promote apoptosis, while others such as Bcl-x_L and Bcl-2 protect against programmed cell death (Adams & Cory, 1998; Minn et al., 1998). The proapoptotic and anti-apoptotic proteins within the Bcl-2 family interact with one another and antagonize each others activities (Yang et al., 1995). We have previously described the 3D structure of the cell survival protein Bcl-x_L (Muchmore et al., 1996) and a Bcl-x_L/Bak peptide complex (Sattler et al., 1997). Bcl-x_L is an all α-helical protein that contains a hydrophobic cleft, which binds to the Bak peptide. When bound to Bcl-x_L, the Bak peptide adopts an amphipathic α-helix. The 3D structure and binding affinities of mutant Bak peptides revealed that complex formation is stabilized by specific hydrophobic and electrostatic interactions.

Reprint requests to: Stephen Fesik, Abbott Laboratories, 100 Abbott Park Rd., D460, AP10, Abbott Park, Illinois 60064-6098; e-mail: stephen.fesik@abbott.com.

Abbreviations: CD, circular dichroism, NTCB, 2-nitro-5-thiocyanatobenzoic acid; NOE, nuclear Overhauser effect; RMSD, root-mean-square deviation; HSQC, heteronuclear single-quantum coherence; NOESY, nuclear Overhauser effect spectroscopy; TOCSY, total correlation spectroscopy; FITC, fluorescein-isothiocyanate; TFE, trifluoroethanol; 3D, three-dimensional.

Another pro-apoptotic protein, Bad, also binds tightly to Bcl-x_L. The region of Bad responsible for binding to Bcl-x_L is homologous to Bak. However, unlike the tight binding observed with the Bak 16-mer, a 16-residue peptide derived from this region of Bad exhibited little or no interaction with Bcl-x_L. To obtain tight binding to Bcl-x_L, it was necessary to extend the length of the Bad 16-mer at both the N- and C-termini. These longer peptides containing 26 amino acids were found to bind tightly to Bcl-x_L with a K_D of ~6 nM (Kelekar et al., 1997; Ottilie et al., 1997). This suggests that Bcl-x_L contains additional binding pockets that were not identified in our previous structural studies of the Bcl-x_L/Bak peptide complex. These additional binding sites on Bcl-x_L may be critical for mediating complex formation with Bad and for conferring the binding specificity observed within the Bcl-2 family of proteins.

To determine the structural features important for formation of the Bcl-x_L/Bad complex, the solution structure of Bcl-x_L complexed with a 25-residue peptide derived from the Bad protein (residues 140–164) was solved. In addition, we measured the binding affinities of mutant Bad peptides to Bcl-x_L to define the relative contributions of the amino acid residues of Bad for binding to Bcl-x_L. Because the peptides that bind to Bcl-x_L adopt an α-helix in the bound state, we also examined the helix propensity of these peptides using CD. From these studies we explain why the Bad 16-mer does not bind, even though it contains most of the key residues in Bak that interact with Bcl-x_L.

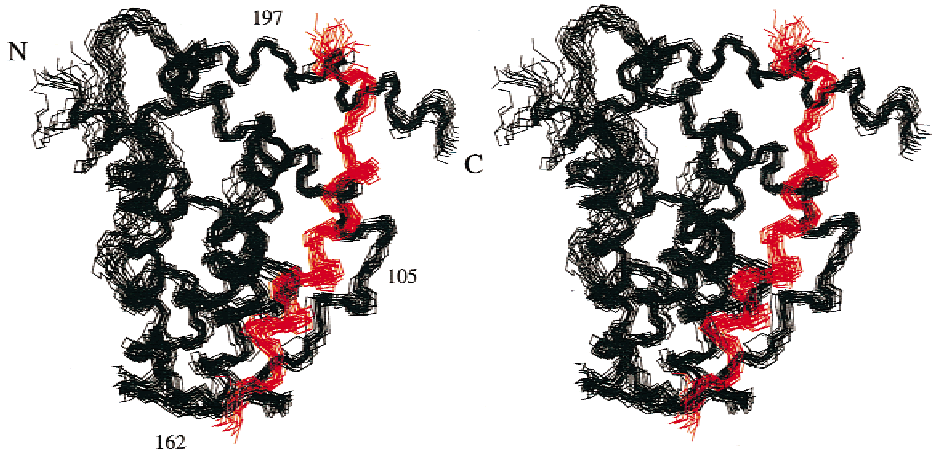

Fig. 1. Stereoview of the backbone atoms (N,Cα,C′) of 20 superimposed NMR-derived structures of the Bcl-x_L/Bad complex. The Bad peptide (residue 140–164 of Bad) is shown in red. PDB acession code: 1G5J.

Results and discussion

Structure determination

A total of 2,475 nontrivial NMR-derived restraints were employed in the structure calculations of the Bcl-x_L/Bad peptide complex. The restraints were derived from 1,904 intramolecular NOEs for Bcl-x_L, 88 intramolecular NOEs for the Bad peptide, 129 intermolecular NOEs, 162 slowly exchanging amide protons, and 192 φ and ψ torsional restraints obtained from chemical shift database searching using the TALOS program (Cornilescu et al., 1999).

The structure of the complex was well defined by the NMR data except for the artificial loop connecting helix 1 and helix 2 (residues 31–44) and a few residues at the N- and C-termini (Fig. 1; Table 1). In the final set of structures, there were no distance violations greater than 0.4 Å, and no dihedral angle violations greater than 5°. In addition, the energy for the van der Waals repulsion term is small (Table 1), indicating that the structures do not contain unfavorable interatomic contacts. The RMSD about the mean coordinate positions for residues 5–30 and 45–210 of Bcl-x_L and 3–20 of the Bad peptide in the ensemble of 20 structures (Fig. 1) was 0.58 ± 0.07 Å for the backbone and 1.11 ± 0.06 Å for all heavy atoms. Analysis of the average, minimized structure with the program PROCHECK-NMR (Laskowski et al., 1996) showed that 94.4% of the residues are in the allowed region of the Ramachandran plot.

Description of the structure

The structure of Bcl-x_L (Fig. 2) consists of eight α-helices connected by loops. Helix 5 is primarily hydrophobic and forms the core of the molecule with the other amphipathic helices sequestering the core from solvent. Although absent in the uncomplexed protein, helix 8 was observed in the complex of Bcl-x_L with the Bad peptide.

The loop connecting helix 1 and helix 2 that has been shortened with respect to the wild-type protein is unstructured in solution as evidenced by the lack of medium- and long-range NOEs for this region. Helix 2 is connected to helix 3 by a single residue, Tyr105, which results in a nearly orthogonal orientation for these two helices. The loops between helix 3 and 4, helix 4 and 5, and helix 5 and 6 consist of 14, 4, and 3 residues, respectively, and in each case, the loops allow a nearly 180° chain reversal.

The binding site for the Bad peptide is a groove lined with hydrophobic side chains formed predominately by helix 2, 3, 4,

Table 1. *Structural statistics for the Bcl-x_L/Bad complex*

	$\langle SA\rangle$[a]	$\langle\overline{SA}\rangle_r$
RMSD from experimental distance restraints (Å)		
Protein (NOEs)		
Intraresidue (654)	0.0076 ± 0.003	0.004
Sequential (421)	0.023 ± 0.002	0.025
Medium range (399)	0.021 ± 0.003	0.019
Long range (430)	0.016 ± 0.001	0.015
Hydrogen bonds (142)	0.021 ± 0.002	0.023
Peptide (NOEs)		
Intraresidue (48)	0.000 ± 0.000	0.000
Sequential (21)	0.001 ± 0.001	0.000
Medium range (14)	0.019 ± 0.016	0.029
Long range (0)		
Intermolecular (129)	0.012 ± 0.002	0.014
Hydrogen bonds (20)	0.047 ± 0.009	0.038
X-PLOR potential energies (kcal mol^{-1})[b]		
E_{tot}	141.1 ± 18.3	196.4
E_{bond}	7.7 ± 0.8	9.1
E_{ang}	105.8 ± 4.0	107.2
E_{imp}	10.2 ± 1.6	8.4
E_{repel}	35.4 ± 3.3	32.4
E_{noe}	2.5 ± 0.8	2.2
$E_{L\text{-}J}$	−1,137.4 ± 19.0	−1,060.9
Cartesian coordinate RMSD (Å)[c]	N, Cα, and C′	All heavy
$\langle SA\rangle$ vs. $\langle\overline{SA}\rangle_r$	0.58 ± 0.07	1.11 ± 0.06

[a] $\langle SA\rangle$ is the ensemble of the 20 lowest enegy structures while $\langle\overline{SA}\rangle_r$ is the energy-minimized mean structure.

[b] $E_{L\text{-}J}$ was not used in the refinement, but is included as an independent assessment of nonbonded geometry.

[c] For residues 5–30, 45–210 of the protein and residues 142–158 of the peptide.

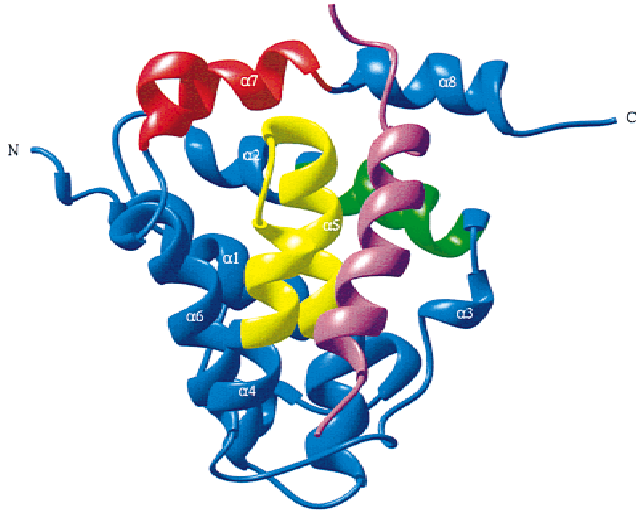

Fig. 2. A Ribbons (Carson, 1987) depiction of the averaged, minimized NMR structure of the Bcl-x_L/Bad complex. The BH1, BH2, and BH3 domains of Bcl-x_L are colored yellow, red, and green, respectively, and the Bad peptide is shown in purple.

and 8, and the four-residue loop connecting helix 4 to helix 5 (Figs. 2, 3). The peptide binds as an amphipathic α-helix from residue 144 to 160 with its hydrophobic side contacting the protein (Fig. 3A). The three residues at the amino-terminus and the five residues at the carboxy-terminus are in an extended conformation with the exception of Phe162, which kinks toward the protein and makes contact with residues in helix 7 and helix 8. The side chains of Tyr147, Leu151, and Phe158 of the peptide are completely sequestered from solvent in the complex. The Tyr147 subsite is composed of side chains from Phe105, Leu108, Val126, Phe146, and Leu150 of Bcl-x_L, while the Leu151 subsite is composed of side chains from Phe97, Ala104, Phe105, Leu130, Ala142, and Phe146. The Phe158 subsite is composed of Ala93, Phe97, Gly138, Val141, and the aliphatic portion of Glu96. The other residues of the peptide that contact the protein (Ala144, Ala145, Met154, Ser155, Val159, and Ser161) are partially exposed to solvent.

Comparison to Bcl-x_L/Bak peptide structure

The overall fold of Bcl-x_L bound to the Bad peptide is very similar to that observed in the BcL-x_L/Bak complex. However, there are some interesting differences at the peptide–protein interface (Figs. 3B, 4). The peptide binding groove of Bcl-x_L is somewhat wider in the Bcl-x_L/Bad complex than in the Bcl-x_L/Bak complex, especially near the amino-terminal end of helix 3. For the bound Bak peptide, this region accommodates a valine residue; whereas, in the Bad peptide, this valine is substituted by a tyrosine. Thus, in binding to the Bad peptide, the groove must open up to accommodate a larger side chain at this position. In addition, helix 3 is distorted in the Bcl-x_L/Bad complex compared to the Bcl-x_L/Bak complex (Figs. 3B, 4). This may be due, at least in part, to the different role played by Phe105 in the two complexes. In the Bcl-x_L/Bak complex, the side chain of Phe105 is pointing away from the core of the protein and interacts with Ile80 and Ile81 of the Bak peptide. In contrast, in the Bcl-x_L/Bad complex, Phe105 is rotated inward and interacts with Tyr147 and Leu151 of the Bad peptide. Thus, in the Bcl-x_L/Bak peptide complex, Phe105 interacts with two partially exposed, aliphatic residues; whereas, in the Bcl-x_L/Bad peptide complex, Phe105 forms an integral part of the binding site for two buried residues.

In addition to the differences between Bcl-x_L/Bak and Bcl-x_L/Bad at the core of the binding site, the longer Bad peptide makes new contacts at both ends of the binding groove. While the amino-terminal asparagine and the Trp142 are completely solvent exposed, Leu141, Ala144, and Ala145 clearly form interactions with the protein. At the carboxy terminus of the Bad peptide, Phe162 interacts with Tyr195, Ala199, and Ser203 of Bcl-x_L.

Mutagenesis of the Bad peptide

To determine which of the additional interactions observed between Bcl-x_L and the N- and C-terminal residues of the Bad peptide are responsible for the increase in binding affinity observed for the Bad 25-mer compared to the Bad 16-mer, the additional residues of the longer Bad peptide were mutated, and the resulting peptides tested for binding to Bcl-x_L (Table 2). When Asn140, Leu141, or Trp142 at the amino terminus of the Bad peptide were mutated to Ala, there was no effect on binding to Bcl-x_L. In fact, a peptide in which all three residues were mutated to alanine still bound tightly to Bcl-x_L (Table 2). Mutation of Ala144 and Ala145 to glycine also does not significantly affect the affinity of these mutant peptides for Bcl-x_L. Similarly, individual mutations of the four carboxy-terminal residues of the Bad peptide to alanine have essentially no effect on the affinity of the Bad peptide for Bcl-x_L. These results suggest that the interactions observed between Bcl-x_L and the N- and C-terminal residues of the Bad peptide observed in the NMR structure of the complex do not contribute to the binding affinity of the longer Bad peptide for Bcl-x_L.

In addition to the mutations discussed above, mutants of the Bad 16-mer were prepared in which individual residues were changed to those found in the Bak peptide. These studies were conducted to explore the possibility that one or more of the Bad residues may

Table 2. *Peptide binding to Bcl-x_L*

Sequence		K_d (nM)[a]
GQVGRQLAIIGDDINR	(Bak 16-mer)	480
QRYGRELRRMSDEFVD	(Bad 16-mer)	50,000
NLWAAQRYGRELRRMSDEFVDSFKK	(Bad 25-mer)	0.6
ALWAAQRYGRELRRMSDEFVDSFKK		0.4
N**A**WAAQRYGRELRRMSDEFVDSFKK		0.7
NL**A**AAQRYGRELRRMSDEFVDSFKK		0.3
AAAAAQRYGRELRRMSDEFVDSFKK		0.5
NLW**G**AQRYGRELRRMSDEFVDSFKK		0.8
NLWA**G**QRYGRELRRMSDEFVDSFKK		2.4
NLWAAQRYGRELRRMSDEFVD**A**FKK		0.3
NLWAAQRYGRELRRMSDEFVDS**A**KK		2.1
NLWAAQRYGRELRRMSDEFVDSF**A**K		1.2
NLWAAQRYGRELRRMSDEFVDSFK**A**		0.2

[a] Measured in a fluorescence polarization competition assay as described in Materials and methods.

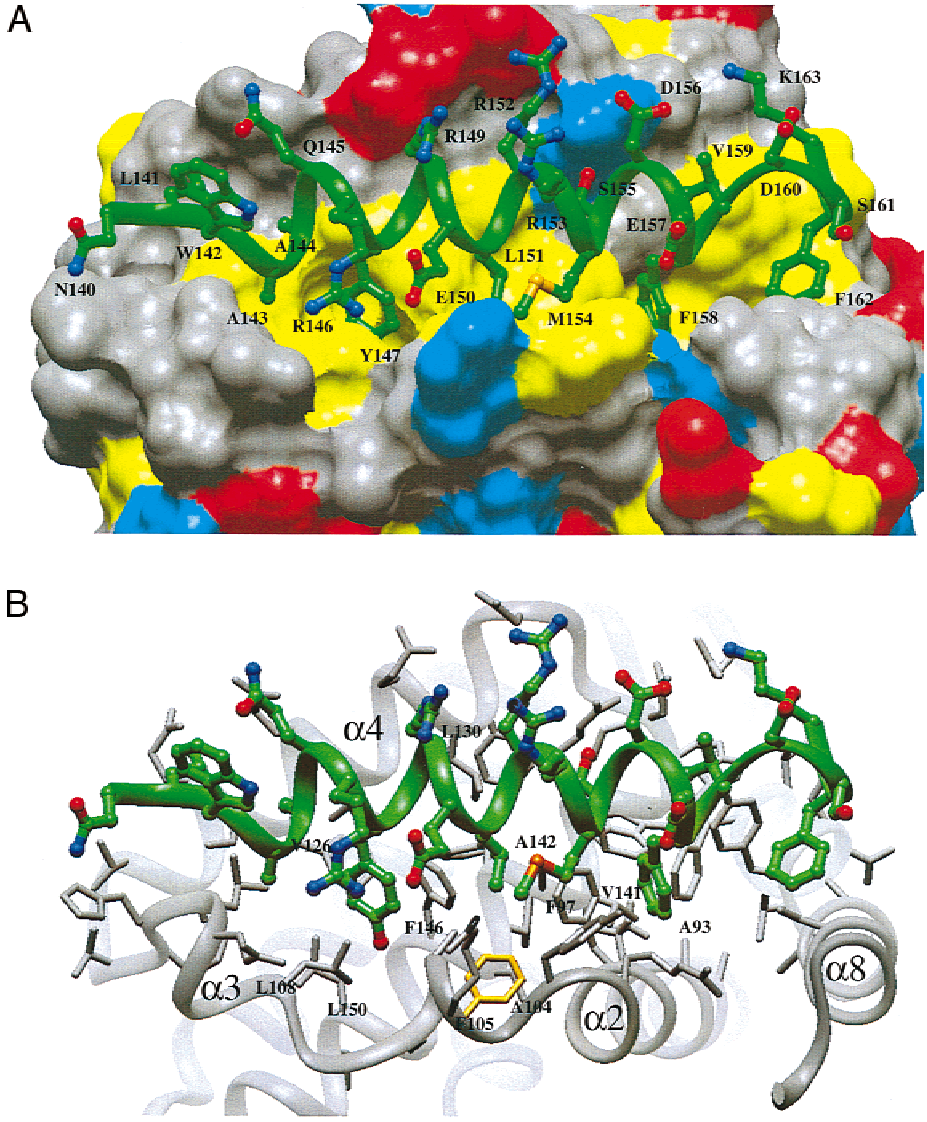

Fig. 3. A: Connolly surface of Bcl-x_L with bound Bad peptide. Valine, leucine, isoleucine, tyrosine, phenylalanine, tryptophan, and alanine side chains of the protein are colored yellow, lysine and arginine side chains are colored blue, glutamate and aspartate side chains are colored red. The residues of the Bad peptide are labeled. **B:** The NMR structure of the Bcl-x_L/Bad peptide complex in which the protein side chains are shown and labeled. Binding site for Bad peptide on Bcl-x_L with selected sidechains of the protein labeled. The side chain of Phe105 is colored orange.

form unfavorable contacts with the protein, which could reduce the binding affinity of the Bad 16-mer compared to the Bak 16-mer. As shown in Table 3, the only mutation with any effect on the affinity of the Bad 16-mer for Bcl-x_L is the substitution of Asp160 with an arginine. One possible explanation for the increase in affinity for the Asp to Arg mutation is that Arg160 forms additional contacts with the protein. However, in the structure of the Bcl-x_L/Bad complex (Fig. 3), Asp160 is solvent exposed and points away from any charged residue of the protein. Therefore, the observed boost in affinity upon changing this residue to an arginine cannot be explained by additional peptide–protein interactions. Another possibility is that Asp160 has a destabilizing effect on helix formation due to its proximity to Asp156 and Glu157 in the bound peptide. Furthermore, the α-helix has a large macrodipole and a negatively charged residue near the carboxy terminus would be expected to have a destabilizing effect (Muñoz & Serrano, 1995a). Therefore, substitution of Asp160 with an arginine may stabilize helix formation and thus explain the increased affinity of the Arg160 mutant peptide for Bcl-x_L.

Helix propensity and peptide design

To test the importance of helix propensity for peptide binding to Bcl-x_L, CD spectra were acquired for various peptides in 30% TFE. From the mean residue ellipticity at 222 nm, the percentage of α-helix was derived and compared to the affinity of each peptide for Bcl-x_L (Table 4). As hypothesized, the Asp160 to Arg mutant possesses a greater helix propensity compared to the wild-type Bad 16-mer, which is consistent with its increase in affinity for Bcl-x_L. Also consistent with our hypothesis are the measurements made on

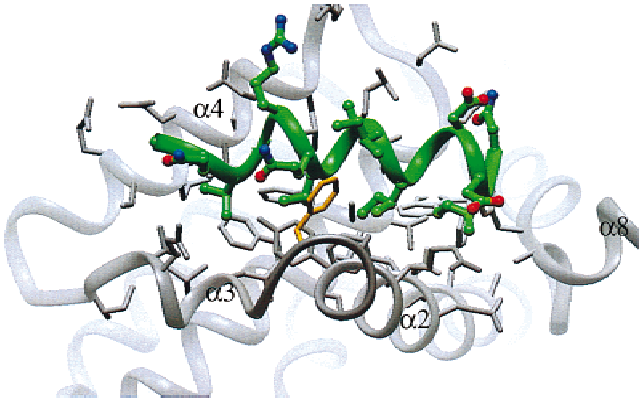

Fig. 4. Binding site for Bak peptide on Bcl-x_L. The side chain of Phe105 is colored orange.

the Bak 16-mer and the Bad 25-mer. Both have a higher helix propensity than the wild-type Bad 16-mer and, as with the Asp160 to Arg mutant, their increased helicity parallels their improved affinity for Bcl-x_L.

To further test the importance of helix propensity for peptide binding to Bcl-x_L, two peptides were designed, based on the Bad 16-mer, with the aim of increasing helix propensity while maintaining the native contacts to the protein. This was accomplished using the program AGADIR (Muñoz & Serrano, 1995a, 1995b) as described under Materials and methods. Tyr147, Leu151, Asp156, Phe158, and Val159, which closely contact the protein, were left intact in both of the designed peptides. Only the solvent-exposed residues that would not be expected to affect the binding affinity were changed. Both peptides were found to have a markedly increased helix propensity compared to the native Bad 16-mer (Table 4). Furthermore, both peptides bind much more tightly to Bcl-x_L than the wild-type Bad 16-mer, suggesting that the ability to form an α-helix is a critical factor for binding to Bcl-x_L.

Conclusions

We have determined the solution structure of a 25-residue peptide from the Bad protein bound to Bcl-x_L to compare its mode of binding to that previously observed for a 16-residue peptide from Bak. To our surprise, the additional interactions observed between the extra residues of the Bad 25-mer and the protein were not responsible for the increased affinity of the Bad 25-mer for Bcl-x_L compared to the Bad 16-mer. Indeed, based on mutagenesis studies, we have shown that these extra residues contributed very little to the increased affinity of the Bad 25-mer for Bcl-x_L. Instead, the increase in affinity of the longer Bad peptide is due to the increase in helix propensity of the 25-mer compared to the 16-mer. To support this conclusion, we designed two 16-residue peptides with high helix propensity, which maintained the native contacts of the Bad peptide with Bcl-x_L. Both peptides bound much more tightly to the protein than the wild-type.

This study clearly demonstrates that the intermolecular contacts in a protein/ligand complex are not always sufficient to explain a ligand's binding affinity. The energetic accessibility of the bound conformation must also be considered. In the case of the Bad 16-mer binding to Bcl-x_L, energetically favorable interactions between the peptide and the protein could not overcome the energetically unfavorable intrapeptide interactions necessary for helix formation. These same considerations can be applied to the design of protein-targeted drug molecules, many of which are highly flexible (Furet et al., 1999; Matthews et al., 1999; Shakespeare et al., 2000). In such cases it may be necessary to consider not only the spatial placement of binding elements, but also the conformational flexibility of the scaffold to which they are attached.

Table 3. *Bad to Bak permutation*

Sequence		K_d (nM)
QRYGRELRRMSDEFVD	(Bad 16-mer)	50,000
GQVGRQLAIIGDDINR	(Bak 16-mer)	480
Q**Q**YGRELRRMSDEFVD		33,000
QR**V**GRELRRMSDEFVD		95,000
QRYGREL**A**RMSDEFVD		280,000
QRYGRELR**I**MSDEFVD		30,000
QRYGRELRR**I**SDEFVD		120,000
QRYGRELRRMSDE**I**VD		190,000
QRYGRELRRMSDEF**N**D		24,000
QRYGRELRRMSDEFV**R**		3,300

Materials and methods

Sample preparation

All studies were conducted using a carboxy-terminal histidine-tagged deletion mutant of Bcl-x_L that lacks the putative carboxy-terminal transmembrane region and residues 49–88, a flexible loop not necessary for antiapoptotic activity (Muchmore et al., 1996). Unlabeled, uniformly ^{15}N, uniformly ^{15}N,^{13}C, and uniformly ^{15}N,^{13}C,75%^{2}H protein samples were prepared by growing *Escherichia coli* strain BL21 (DE3) that overexpresses this protein. All Bcl-x_L samples were purified by affinity chromatography on Ni-NTA resin (Novagen, Madison, Wisconsin). The Bad 25-mer corresponds to residues 140–164 of the Bad protein, and the Bak 16-mer corresponds to residues 72–87 of the Bak protein (Kelekar et al., 1997).

Unlabeled peptides were obtained from SynPep Corporation (Dublin, California) at a purity of >90% and were used without further purification. Uniformly ^{15}N and ^{15}N,^{13}C-labeled Bad peptides were prepared as a fusion protein with the N-terminal end of the CARD domain from RAIDD, followed by thiocyanylation-alkaline cleavage of the fusion protein according to the protocol of Stark (1977). The cleavage efficiency was about 70–80% and the peptide obtained in this way did not contain any modified residues. The following 1:1 complexes were prepared at concentrations of 0.5–1.0 mM in a 40 mM sodium phosphate buffer (pH 7.0) in $^{2}H_2O$ or $H_2O/^{2}H_2O$ (9:1): ^{15}N-Bcl$^{-x_l}$/unlabeled Bad, ^{15}N,^{13}C-Bcl$^{-x_l}$/unlabeled Bad, ^{15}N,^{13}C,75%^{2}H-Bcl$^{-x_l}$/unlabeled Bad, unlabeled Bcl$^{-x_l}$/^{15}N-Bad, unlabeled Bcl$^{-x_l}$/^{15}N,^{13}C-Bad.

NMR spectroscopy

NMR spectra were acquired at 30 °C on Bruker spectrometers operating at proton field strengths of 500, 600, and 800 MHz. The

Table 4. *Affinity vs. helix propensity*

Sequence		K_d (nM)	%Helix in 30% TFE
QRYGRELRRMSDEFVD	(Bad 16-mer)	50,000	7
QRYGRELRRMSDEFV**R**		3,300	13
GQVGRQLAIIGDDINR	(Bak 16-mer)	480	22
NLWAAQRYGRELRRMSDEFVDSFKK	(Bad 25-mer)	0.6	44
Q**QY**A**R**ELR**IMA**DEFV**R**		439	28
DDYA**R**ELR**MMA**DEFV**R**		203	46

backbone resonances of Bcl-x_L in the complex were assigned from a suite of deuterium-decoupled triple resonance experiments [HNCA, HN(CO)CA, HNCO, HN(CA)CO, CBCANH, CBCA(CO)NH] on a ^{15}N, ^{13}C, ^{2}H-labeled protein bound to unlabeled peptide (Yamazaki et al., 1994). The side-chain signals were assigned from HCCH-TOCSY, HC(CO)NH-TOCSY, HACACO, and ^{15}N-edited TOCSY experiments (Bax et al., 1990; Logan et al., 1992; Montelione et al., 1992; Grzesiek & Bax, 1993). Stereospecific assignments of the Leu and Val methyl groups were obtained using the biosynthetic approach described by Wüthrich and co-workers (Neri et al., 1989). The backbone resonances of the peptide were assigned from HNCA, HN(CO)CA, CBCANH, CBCA(CO)NH experiments on ^{15}N,^{13}C peptide bound to unlabeled protein. Side-chain assignments for the bound peptide were obtained from 2D TOCSY and NOESY experiments. Intramolecular proton–proton distance restraints were obtained from 3D ^{15}N-edited NOESY and ^{13}C-edited NOESY experiments acquired with a mixing time of 80 ms on both the samples with labeled protein and the samples with labeled peptide (Fesik & Zuiderweg, 1988). Intermolecular distance restraints were also obtained from these NOESY experiments and from a 3D ^{13}C-edited(ω_1),^{12}C-selected(ω_3) NOESY experiment recorded on the sample of uniformly ^{15}N,^{13}C labeled Bcl-x_L bound to unlabeled peptide. Slowly exchanging amide protons were identified by recording a series of 2D ^{1}H/^{15}N HSQC spectra at increasing times after exchanging the samples into $^{2}H_2O$. These studies were conducted with the unlabeled Bad peptide bound to ^{15}N-Bcl-x_L or ^{15}N-labeled Bad peptide bound to unlabeled Bcl-x_L.

Structure calculations

Structures were calculated for the Bcl-x_L/Bad peptide complex using torsional angle dynamics (Stein et al., 1997) followed by simulated annealing with a modified version of the X-PLOR program (Brünger, 1992). The calculations employed 2,121 NOE-derived proton–proton distance restraints, 162 hydrogen bond restraints, and 192 φ and ψ torsional restraints obtained from an analysis of the C′, N, Cα, Hα, and Cβ chemical shifts using the TALOS program (Cornilescu et al., 1999). Based on intensity, the NOE-derived restraints were placed into one of four upper-bound categories (3.0, 4.0, 5.0, or 6.0 Å).

Circular dichroism

Peptides were dissolved in 40 mM sodium phosphate buffer, 30% TFE, pH 7.0, at a concentration of ~0.1 mg/mL. CD measurements were acquired at room temperature using a JASCO model J-715 spectropolarimeter with a 0.3 cm cuvette. The CD signal at 222 nm, after subtracting the blank, was converted to mean residue ellipticity, $[\theta]_{obs}$, using the equation:

$$[\theta]_{obs} = 100[\theta]_{222}/Cnl$$

where C is the peptide concentration in millimolarity, n is the number of residues in the peptide, and l is the pathlength in centimeters.

Percent helix was then derived using the following equation:

$$\%\ \text{helix} = [\theta]_{obs} - [\theta]_{coil}/[\theta]_{helix} - [\theta]_{coil}$$

where $[\theta]_{helix}$ is the mean residue ellipticity for a complete helix, i.e., $-42{,}500(1 - (3/n))$, and $[\theta]_{coil}$ is the ellipticity for a complete random coil, i.e., $+640$ (Rohl et al., 1996; Meyers et al., 1997).

Fluorescence spectroscopy

The relative affinity of each peptide for Bcl-x_L was determined using a fluorescence polarization-based competitive binding assay with a fluorescein-labeled Bad peptide NLWAAQRYGRELRR MSDK(FITC)KFVD (Synpep Corporation, Dublin, California). The dissociation constant of this fluoresceinated peptide from Bcl-x_L is ~30 nM.

All titrations were automated by means of an Abbott clinical diagnostics instrument (IMx, FPIA mode), modified with a special protocol for performing titrations. A complete twofold dilution series, comprised of 20 separate 2 mL samples, was obtained by delivering appropriate individual aliquots to the first seven tubes, aliquots from an intermediate diluted stock for the next seven, and one more intermediate dilution for the final six. Dilution buffer for all stocks and samples was 120 mM sodium phosphate at pH 7.55 with 0.01% bovine gamma globulin and 0.1% sodium azide. The concentrations of the DMSO stock solutions of the peptide were 1–4 mM, as determined by Trp absorbance (O.D. 280 nm), Tyr absorbance (O.D. 293), or amino acid analysis. The final DMSO concentration for all samples never exceeded 1%. Twenty 1.8 μL samples were prepared without fluoresceinated peptide and read as blanks. To each tube, 0.2 μL of a Bcl-x_L, fluoresceinated peptide mixture was added; the tubes were incubated for 5 min at 35 °C, and then read for total intensity and polarization. Free and bound values for the fluoresceinated peptide were constant within a range ±5 mP. Final Bcl-x_L concentration was 114 nM. Comparisons with other, lower Bcl-x_L concentrations, were made for the wild-

type Bad peptide. Additional controls using buffer lacking BGG showed that nonspecific binding to BGG was negligible.

Steady-state polarization data can be analyzed to extract the fractions of bound and free fluorescent ligand owing to the linear additivity of their anisotropy values, weighted by their respective fractional intensities (Lakowicz, 1983). Nonlinear least-squares curve fitting of titration data to a model for simple equilibrium binding of the fluoresceinated peptide to Bcl-x_L was accomplished by programming standard binding equations, solved in terms of bound, free, and observed anisotropy values, into the model development program MINSQ (V. 4.03, Micromath Scientific Software). To determine affinities of nonfluorescent peptides, the analytical approach for equilibrium competition binding taken by Dandliker and co-workers was used, again employing MINSQ for fitting of titration curves (Dandliker et al., 1981). Confirmation of the validity of these experimental and fitting procedures was obtained by comparing results after performing fluoresceinated peptide binding and competition binding titrations at different fixed Bcl-x_L or fluoresceinated peptide concentrations.

Peptide design

Individual residues of the Bad 16-mer, which are not involved in protein binding, were sequentially modified with in-house written software, and each mutant peptide was then evaluated for helix propensity using the program AGADIR (Muñoz & Serrano, 1995a, 1995b). Once the optimal residues were determined for each position, adjustments were made to maintain the overall charge balance and amino acid diversity of the peptide, while still maintaining total helicity.

References

Adams JM, Cory S. 1998. The Bcl-2 protein family: Arbiters of cell survival. *Science 281*:1322–1325.

Bax A, Clore GM, Gronenborn AM. 1990. ^{1}H-^{1}H correlation via isotropic mixing of ^{13}C magnetization, a new three-dimensional approach for assigning ^{1}H and ^{13}C spectra of ^{13}C-enriched proteins. *J Magn Reson 88*:425–431.

Brünger AT. 1992. *X-PLOR version 3.1 manual*. New Haven, Connecticut: Yale University Press.

Carson M. 1987. Ribbon models of macromolecules. *J Mol Graphics 5*:103–106.

Cornilescu G, Delaglio F, Bax A. 1999. Protein backbone angle restraints from searching a database for chemical shift and sequence homology. *J Biomol NMR 13*:289–302.

Dandliker WB, Hsu ML, Levin J, Rao BR. 1981. Equilibrium and kinetic inhibition assays based upon fluorescence polarization. *Methods Enzymol 74*:3–28.

Fesik SW, Zuiderweg ERP. 1988. Heteronuclear three-dimensional NMR spectroscopy. A strategy for the simplification of homonuclear two-dimensional spectra. *J Magn Reson 78*:588–593.

Furet P, García-Echeverria C, Gay B, Schoepfer J, Zeller M, Rahuel J. 1999. Structure-based design, synthesis, and X-ray crystallography of a high-affinity antagonist of the Grb2-Sh2 domain containing an asparagine mimetic. *J Med Chem 42*:2358–2363.

Grzesiek S, Bax A. 1993. The orign and removal of artifacts in 3D HCACO spectra of proteins uniformly enriched with ^{13}C. *J Magn Reson Series B 102*:103–106.

Kelekar A, Chang BS, Harlan JE, Fesik SW, Thompson CB. 1997. Bad is a BH3 domain-containing protein that forms an inactivating dimer with Bcl-xL. *Mol Cell Biol 17*:7040–7046.

Lakowicz JR. 1983. *Principles of fluorescence spectroscopy*. New York: Plenum Press.

Laskowski RA, Rullmann JA, MacArthur MW, Kaptein R, Thornton JM. 1996. AQUA and PROCHECK-NMR: Programs for checking the quality of protein structures solved by NMR. *J Biomol NMR 8*:477–486.

Logan TM, Olejniczak ET, Xu RX, Fesik SW. 1992. Side chain and backbone assignments in isotopically labeled proteins from two heteronuclear triple resonance experiments. *FEBS Lett 314*:413–418.

Matthews DA, Dragovich PS, Webber SE, Fuhrman SA, Patick AK, Zalman LS, Hendrickson TF, Love RA, Prins TJ, Marakovits JT, et al. 1999. Structure-assisted design of mechanism-based irreversible inhibitors of human rhinovirus 3C protease with potent antiviral activity against multiple rhinovirus serotypes. *Proc Natl Acad Sci USA 96*:11000–11007.

Meyers JK, Pace CN, Scholtz JM. 1997. Helix propensities are identical in proteins and peptides. *Biochemistry 36*:10923–10929.

Minn AJ, Swain RE, Ma A, Thompson CB. 1998. Recent progress on the regulation of apoptosis by Bcl-2 family members. *Adv Immunol 70*:245–279.

Montelione GT, Lyons BA, Emerson SD, Tashiro M. 1992. An efficient triple resonance experiment using carbon-13 isotropic mixing for determining sequence-specific resonance assignments of isotopically-labeled proteins. *J Am Chem Soc 114*:10974–10975.

Muchmore SW, Sattler M, Liang H, Meadows RP, Harlan JE, Yoon HS, Nettesheim D, Chang BS, Thompson CB, Wong SL, et al. 1996. X-ray and NMR structure of Human Bcl-x_L, an inhibitor of programmed cell death. *Nature 381*:335–341.

Muñoz V, Serrano L. 1995a. Elucidating the folding problem of helical peptides using empirical parameters, II: Helix macrodipole effects and rational modification of the helical content of natural peptides. *J Mol Biol 245*:275–296.

Muñoz V, Serrano L. 1995b. Elucidating the folding problem of helical peptides using empirical parameters, III: Temperature and pH dependence. *J Mol Biol 245*:297–308.

Neri D, Szyperski T, Otting G, Senn H, Wüthrich K. 1989. Stereospecific nuclear magnetic resonance assignments of the methyl groups of valine and leucine in the DNA-binding domain of the 434 repressor by biosynthetically directed fractional ^{13}C labeling. *Biochemistry 28*:7510–7516.

Ottilie S, Diaz JL, Horne W, Chang J, Wang Y, Wilson G, Chang S, Weeks S, Fritz LC, Oltersdorf T. 1997. Dimerization properties of human Bad—Identification of a BH-3 domain and analysis of its binding to mutant Bcl-2 and Bcl-x_L proteins. *J Biol Chem 272*:30866–30872.

Rohl CA, Chakrabartty A, Balwin RL. 1996. Helix propagation and N-cap propensities of the amino acids measured in alanine-based peptides in 40 volume percent trifluoroethanol. *Protein Sci 5*:2623–2637.

Sattler M, Liang H, Nettesheim D, Meadows RP, Harlan J, Eberstadt M, Yoon HS, Shuker SB, Chang BS, Minn AJ, et al. 1997. Structure of Bcl-x_L–Bak peptide complex: Recognition between regulators of apoptosis. *Science 275*:983–986.

Shakespeare W, Yang M, Bohacek R, Cerasoli F, Stebbins K, Sundaramoorthi R, Azimioara M, Vu C, Pradeepan S, Metcalf C III, et al. 2000. Structure-based design of an osteoclast-selective, nonpeptide Src homology 2 inhibitor with in vivo antiresorptive activity. *Proc Natl Acad Sci USA 97*:9373–9378.

Stark GR. 1977. Cleavage at cysteine after cyanylation. *Methods Enzymol 47*:129–132.

Stein EG, Rice LM, Brünger AT. 1997. Torsiona angle molecular dynamics: a new efficient tool for NMR structure calculation. *J Magn Reson Ser B 124*:154–164.

Yamazaki T, Lee W, Arrowsmith CH, Muhandiram DR, Kay LE. 1994. A suite of triple resonance NMR experiments for the backbone assignment of ^{15}N, ^{13}C, ^{2}H labeled proteins with high sensitivity. *J Am Chem Soc 116*:11655–11666.

Yang E, Zha J, Jockel J, Boise LH, Thompson CB, Korsmeyer SJ. 1995. Bad, a heterodimeric partner for Bcl-xL and BcL-2, displaces Bax and promotes cell death. *Cell 80*:285–291.